

UN  
82  
F3765  
2607

**SPECTROSCOPIC ANALYSIS OF OXYGEN SENSING AEROGELS**

By

**John R. Ferrarone**

\*\*\*\*\*

Submitted in partial fulfillment  
of the requirements for  
Honors in the Department of Chemistry

UNION COLLEGE

June, 2007

## ABSTRACT

FERRARONE, JOHN R. Spectroscopic Analysis of Oxygen Sensing Aerogels.

Department of Chemistry, June 2007

An aerogel is highly porous solid that is comprised of 90-99% air. Aerogels can be doped with probe molecules that act as sensors of certain gases. The porous matrix of aerogels makes them suitable platforms for studying the sensing capabilities of different probe molecules. In this study, we created oxygen sensing, silica-based aerogels, using tetramethyl orthosilicate (TMOS) for the matrix precursor and platinum tetra(pentafluorophenyl)porphine (PtTFPP) as the probe. We then used fluorescence spectroscopy to examine the PtTFPP-doped aerogels in different environments. The sensing ability of PtTFPP was then compared to platinum (II) octaethylporphine (PtOEP), another oxygen sensing probe. In 100 percent nitrogen, we found that the PtTFPP-doped aerogel produced a peak at 650 nm, whereas PtOEP produced a peak at 646 nm. A time-based scan, in which the proportions of air and nitrogen in the aerogel's environment were varied, also revealed that the interaction between oxygen and PtTFPP was reversible. The luminescence lifetimes of PtTFPP and PtOEP were also compared.

## Table of Contents

<b>Abstract</b>	<b>iii</b>
<b>Table of Figures</b>	<b>iv</b>
<b>Table of Tables</b>	<b>v</b>
<b>Introduction</b>	<b>1</b>
<b>Experimental</b>	<b>9</b>
Preparation of PtTFPP- and PtOEP-doped Sol-Gels	9
Rapid Supercritical Extraction	10
Fabrication with Other Molds	12
Luminescence Measurements	16
Time-based Luminescence Scans	16
Luminescence Lifetime Scans	17
<b>Results and Discussion</b>	<b>19</b>
Producing Uniform Samples	19
Time-Based Luminescence Scans of Aerogels Produced Via the RSCE Method	27
Time-Based Luminescence Scans of Aerogels Produced Via the Conventional (Autoclave) Method	33
Luminescence Lifetime Studies	37
<b>Conclusions</b>	<b>42</b>
<b>Acknowledgements</b>	<b>44</b>

## Table of Figures

<u>Figure</u>	<u>Title</u>	<u>Page</u>
1-1	Structures of PtOEP and PtTFPP	4
1-2	Schematic of sol-gel, aerogel, and xerogel matrices	5
1-3	Schematic of hot press, mold, and gasket materials	7
2-1	Side view of the closed bottom mold	10
2-2	Schematic of hot press, mold, and gasket materials	11
2-3	Diagram of the square, steel mold	13
2-4	Top view of the round, steel mold	15
3-1	Time-based scan of Phillips' 2-28-06 standard recipe PtOEP-doped aerogels	20
3-2	Time-based scan of 1-20-07 PtOEP-doped aerogels produced in the round mold	22
3-3	Time-based scan of 2-3-07 PtTFPP-doped aerogels produced in closed bottom mold	25
3-4	Time-based scan of 2-10-07 PtOEP-doped aerogel sample 1a	28
3-5	Time-based scan of 2-10-07 PtTFPP-doped aerogel sample 1a	28
3-6	S-V plot of 2-10-07 PtOEP-doped aerogel sample 1a	30
3-7	S-V plot of 2-10-07 PtTFPP-doped aerogel sample 1a	31
3-8	S-V plot of 2-4-07 PtOEP-doped aerogel sample 1 produced in autoclave	35
3-9	Luminescence decay scan for 2-10-07 PtOEP aerogel sample 1a	38
3-10	Luminescence decay scan for 2-10-07 PtTFPP aerogel sample 1a	39

## Table of Tables

<u>Table</u>	<u>Title</u>	<u>Page</u>
2-1	Standard recipe used to produce p-doped sol-gels	9
2-2	The parameters used for the closed bottom mold in the hot press	11
2-3	The parameters used for the square mold in the hot press	14
2-4	The parameters used for the round mold in the hot press	15
2-5	The parameters used for varying O <sub>2</sub> concentration during the anneal of the p-doped aerogels	17
3-1	E <sub>g</sub> F ratios of Phillips' 2-28-06 standard reciped PtOEP-doped aerogels	20
3-2	E <sub>g</sub> F ratios of 1-28-07 PtOEP-doped aerogels produced in the round mold	22
3-3	E <sub>g</sub> F ratios of 2-10-07 PtOEP-doped aerogels produced in the closed bottom mold	23
3-4	E <sub>g</sub> F ratios of 2-3-06 PtTFPP-doped aerogels	25
3-5	E <sub>g</sub> F ratios of 2-10-07 PtTFPP-doped aerogels produced using volume control	26
3-6	Summary of S-V data for 2-10-07 PtOEP-doped aerogels	32
3-7	Summary of S-V data for 2-10-07 PtTFPP-doped aerogels	32
3-8	E <sub>g</sub> F ratios of 2-4-07 PtOEP-doped aerogels produced in the anneal	33
3-9	E <sub>g</sub> F ratios of 2-1-07 PtTFPP-doped aerogels produced in the anneal	34
3-10	Summary of S-V data for 2-4-07 PtOEP-doped aerogels	36
3-11	Summary of S-V data for 2-1-07 PtTFPP-doped aerogels	36
3-12	Luminescence lifetime data for 2-10-07 PtOEP-doped aerogels	40



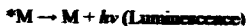
## **Introduction**

An aerogel is a highly porous material that is comprised of 90-99 % air by volume [1]. Nanosized pores give the aerogel many unique properties including an extraordinarily large surface area, and the lowest known density and thermal conductivity of any other solid [1,2]. These properties have resulted in the application of aerogels in batteries, insulation, and nuclear waste storage [1].

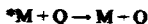
In batteries, aerogels are used gather a large amount of ions in a small area [1]. As a result, a more powerful battery can be condensed into a smaller package. The extremely low thermal conductivity of aerogels also makes these materials an excellent candidate for insulation. The small compartments within the matrix restrict the flow of air through the aerogel, which in turn minimizes the conduction of heat [3]. This property has resulted in the incorporation of aerogels in clothing, electronics, and even space shuttles [1]. This matrix can also be used to trap radioactive materials, making them useful for storing nuclear waste [1].

Another application of aerogels has been their use as platforms for oxygen-sensing molecules. During fabrication, the O<sub>2</sub>-sensing molecule, or "probe," is either covalently attached to, or entrapped within, the aerogel matrix. Thus, the probe becomes securely anchored to aerogel's nanostructure. Since aerogels are highly porous, gases like oxygen can diffuse rapidly through the matrix [4, 5]. Aerogels can be fabricated from silica precursors, such as tetramethoxysilane (TMOS). Silica-based aerogels are sufficiently translucent to allow for optical monitoring of the probe's response to changing environmental conditions [1].

Typically, the response of these probes in an environment is based on luminescence. Luminescence results when the absorption of a photon raises an electron to a higher orbital thereby promoting the molecular species to its excited state. Upon the return of the molecule to its ground state, energy is emitted in the form of heat and light. The following equations represent these properties of luminescence:



where  $M$  is the reporter molecule,  ${}^*M$  is the molecule in the excited state, and  $h\nu$  represents heat and light [6]. In some molecules, luminescence is decreased, or "quenched" in the presence of oxygen. Specifically, the oxygen reduces the amount of molecular species in the excited state. This gives rise to the equation



where  $Q$  represents the quencher, such as oxygen. By using a luminescence spectrometer, the luminescence of a probe-doped aerogel can be measured. Depending on the sensitivity of the probe, the exposure of the aerogel to oxygen can result in a reduction or a complete loss of luminescence intensity (signal on the luminescence spectrum). The response of an oxygen-sensitive probe to varying concentrations of oxygen can be described by the Stern-Volmer (SV) equation for a single molecule in a single microenvironment (the matrix of the aerogel). The equation is written as follows:

$$I_0/I = 1 + K_{SV}[O_2] \quad (1)$$

where  $I_0$  is the intensity of the signal in the absence of the quencher,  $I$  is the signal in the presence of the quencher,  $K_{SV}$  is the SV constant, and  $[O_2]$  is the concentration of the



quencher, oxygen [7]. Through the SV equation, it becomes possible to quantify the sensitivity of a probe to the presence of oxygen.

Ideally, the response of a probe to oxygen concentration is linear, as described by equation (1). In reality, many oxygen sensors do not exhibit a linear response to quencher concentration. This can be due to static quenching, where the quencher interacts with ground state molecules, thereby prohibiting the probe from reaching an excited state [1]. Furthermore, short lifetimes and probes entrapped in different microenvironments within the matrix will also cause the response to be non-linear [1]. To account for multiple microenvironments, a two-site SV equation is used to quantify sensitivity in probes that experience two or more microenvironments. The two-site SV model is written as follows:

$$I_0/I = 1/[(f/(1 + K_{SV1})) + ((1 - f)/(1 + K_{SV2}[O_2]))] \quad (2)$$

where  $f$  is the fraction of the probe in one microenvironment, and  $K_{SV1}$  and  $K_{SV2}$  are the SV constants of their respective microenvironments [7a].

Oxygen-sensing probes have become increasingly important in blood gas analysis, pressure-sensitive paints, combustion, environmental monitoring, and in a variety of other fields [2, 6]. As a result, much of the work with reporter molecules has been focused on the development of new  $O_2$  probes. Among the molecular probes that have received the most attention are Ru(II) and Pt(II)/Pd(II) porphyrin complexes [6]. Figure 1-1 (below) shows the structures of two of the platinum complexes.

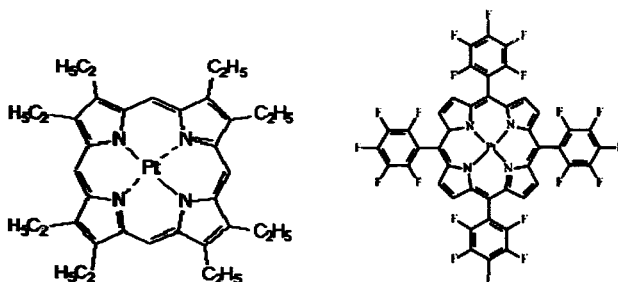


**Figure 1-1: The structures of platinum(II) octaethyl porphyrin (PtOEP) (left) and pentafluorophenyl porphyrin platinum(II) (PtTFPP) (right) [6]. The +2 charges on each structure are not shown.**

In the quenching of these complexes, an O<sub>2</sub> molecule interacts with the metal center to reduce the amount of molecular species that are promoted into the excited state, thereby reducing luminescence. PtOEP has been shown to be an especially sensitive reporter molecule, as its emission intensity decreases substantially with increasing oxygen concentrations [8]. In contrast, Ru(II) complexes have shown to be far less sensitive to changing oxygen pressure [7]. Furthermore, in order to study these probes via luminescence spectroscopy, it is necessary to anchor these molecules to a scaffold, such as the matrix of an aerogel.

An aerogel matrix can be formed using a variety of precursors including carbon, aluminum, and silica based compounds [1]. These precursors form a solid sol-gel matrix via a polymerization reaction. After gelation, the pores in the sol-gel matrix are filled with a liquid solvent mixture. To create an oxygen-sensing aerogel, a probe must be

incorporated in the matrix, either through covalent bonds or by simply entrapping the molecules within the aerogel's pores [4, 5]. By doping the solvent with a reporter molecule, the probe becomes incorporated into the sol-gel matrix during the polymerization reaction. In order to remove the solvent and create an aerogel, the liquid in the pores must be brought above its supercritical point. At that point, the surface tension of the solvent is eliminated, so the liquid can be removed without causing the pores of the matrix to collapse. If the solvent were allowed to evaporate on its own, the sol-gel matrix would condense to form what is known as a xerogel. A schematic of wet sol-gel, aerogel, and xerogel matrices is shown in Figure 1-2.

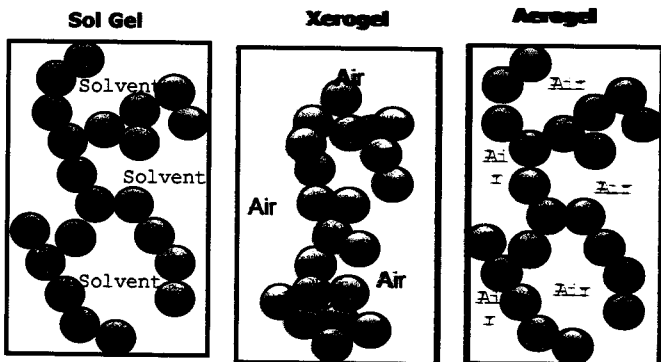


Figure 1-2: A schematic of wet sol-gel, aerogel, and xerogel matrices [9].

There are several methods for supercritical solvent extraction in sol-gels. One method involves exchanging the solvent in the pores for liquid CO<sub>2</sub> and drying the gel in an autoclave. By applying an extremely high pressure to the sol-gel's environment, the supercritical point of the CO<sub>2</sub> solvent is reached. At this point, the solvent can be extracted, leaving an intact aerogel matrix. However, there are several drawbacks to this form of drying. First, the sol-gel must be prepared for the autoclave through a series of time-consuming solvent exchanges. The purpose of the solvent exchange is to replace precursor solvent with one that has a lower supercritical point. The supercritical temperature and pressure for methanol is 512.6 K and 79.8 atm whereas CO<sub>2</sub> has a supercritical temperature and pressure of 304.3 K and 72.8 atm. However, the autoclave must reach potentially dangerous pressure levels in order to reach to the supercritical point of the solvent. In addition, repeated solvent exchanges can flush the probe from the sol-gel if it isn't covalently linked to the matrix [1].

Another technique, known as the Union College rapid supercritical extraction (RSCE), involves preparing the reaction mixture in a one-piece mold [2]. A hydraulic hot press is then used to apply temperature and pressure to this mold in order to achieve the supercritical point of the solvent. Applying heat in the RSCE method also serves to speed up the polymerization reaction [2]. Once the supercritical point is reached, the hot press depressurizes slightly, allowing the supercritical fluid to escape the mold. A schematic of the mold used in the RSCE method is shown in Figure 1-3.

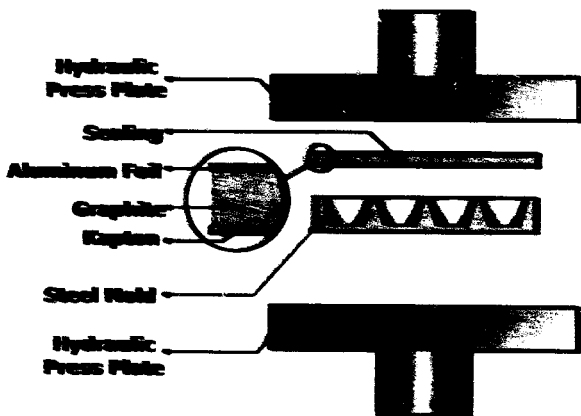


Figure 1-3: A diagram of the mold and gasket materials used in the BSCE method of preparing aerogels [2].

The main advantage that the BSCE method offers over the autoclave method is that the hot press can produce aerogels in a matter of hours, whereas the autoclave technique can take days to weeks depending on the size of the aerogel [2]. However, the BSCE method requires the use of higher temperatures, which can lead to oxide decomposition.

In this study, Pt(IV)- and Pd(II)-doped aerogels were produced using BSCE and autoclave methods. Luminescence spectroscopy was first used to measure and compare the signals of each of these aerogels over a range of oxygen concentrations. The signals produced by Pt(IV)- and Pd(II)-doped aerogels were also compared to those of the aerogels.

1. Pierre, A. C.; Pajonk, G. M. *Chem. Rev.*, 2002, 102, 4243-65.
2. Gauthier, B. M.; Bakrania, S. D.; Anderson, A. M.; Carroll, M. K. *J. Non-Cryst. Solids*, 2004, 350, 238-43.
3. Yoldas, B. E.; Annen, M. J.; Bostaph, J. *Chem. Mater.*, 2002, 12, 2475-84.
4. Plata, D. L.; Briones, Y. J.; Wolfe, R. L.; Carroll, M. K.; Bakrania, S. D.; Mandel, S. G.; Anderson, A. M. *J. Non-Cryst. Solids*, 2004, 350, 326-35.
5. Levantis, N.; Elder, I. A.; Rolison, D. R.; Anderson, M. L.; Merzbacher, C. I. *Chem. Mater.*, 1999, 11, 2837.
6. Demas, J. N.; DeGraff, B. A.; Coleman, P. B. *Anal. Chem.*, 1999, 71, 793A-800A.
7. Kose, M. E.; Carroll, B. F.; Schanze, K. S. *Langmuir*, 2005, 21, 9121-29.
- 7a. J. N. Demas, B. A DeGraff, W. Xu, *Anal. Chem.* 1995, 67, 1377.
8. Lee, S. K.; Okura, I. *Analyst*, 1997, 122, 81.
9. Lax, E. Spectroscopic investigation of the microenvironments experienced by rhodamine probes entrapped in silica aerogels and xerogels. Union College, June, 2005.

## Experimental

### Preparation of PtTFPP and PtOEP-doped Sol-Gels

The precursor recipe for the probe-doped sol-gels was as follows:

Precursor	Volume (mL)
Tetramethyl orthosilicate (TMOS)	8.50
Probe-doped MeOH solution	27.5
Distilled water	3.60
1.5 M Ammonium hydroxide	0.135

Table 2-1: The standard recipe used to produce probe-doped sol-gels.

Tetramethyl orthosilicate (TMOS) was purchased from Sigma-Aldrich at 98% purity.

PtOEP was purchased from Frontier Scientific and used without further purification. The

MeOH was purchased from Frontier Scientific at 99.9% purity.

The PtOEP-doped MeOH solution was made by dissolving 0.0200 g of PtOEP in a liter of methanol. After mixing, 10 mL of this solution was pipetted into a 250-mL volumetric flask and then filled to the mark with methanol. The final concentration of the PtOEP-doped MeOH solution was  $1.00 \times 10^{-6}$  M.

The PtTFPP/MeOH solution was also made by dissolving 0.0200 g of PtTFPP in a liter of methanol. Next, 10 mL of this solution was pipetted into a 250-mL volumetric flask and filled to the mark with methanol. The final concentration of the PtTFPP-doped MeOH solution was  $6.85 \times 10^{-7}$  M.

Each probe-doped stock solution was used to prepare a batch of aerogels (for a total of two batches). The recipe in Table 1 was used to prepare the precursor mixture. Before this mixture was placed in the mold, it was sonicated for approximately 10 min. In

addition, this precursor mixture was used to produce xerogels. To make the xerogels, 4 mL aliquots of the precursor mixture were pipetted into polystyrene cuvettes, and the cuvettes were capped. The sol-gel was allowed to dry under ambient conditions, causing the gels to shrink to about a third of their original height over a period of 1-2 weeks [2].

#### *Rapid Supercritical Extraction*

To obtain the aerogel from the sol-gel, the Union College Rapid Supercritical Extraction (RSCE) drying technique was used. First, a steel mold with a closed-bottom (designed by Smitesh Bakrania) was filled with the precursor mixture. Only the inner four cavities of the mold were used in an attempt to minimize the spectroscopic variation among the gels due to local variations of temperature and pressure within the hot press. Essentially, the inner four cavities were the same distance from the center and the edges of the mold, and thus represented what we believed were similar environments. To maintain control over the volume of the precursor mixture in the mold, 4.50 mL of the mixture was carefully pipetted into each cavity. The design of the mold used can be seen in Figure 2-1 below.



Figure 2-1: A side view of the closed-bottom mold used in the RSCE drying technique. The mold consists of 16 wells arranged in a 4 well by 4 well fashion [1].



Next, one layer each of Kapton, graphite, and then aluminum foil was placed over the top of the steel mold, in that order. The layers of graphite and Kapton act to seal the mold while it is in the hot press. The aluminum foils prevents the graphite from adhering to the hot press after drying has been completed. Figure 2-2 below illustrates the setup for the mold and the gasket materials in the hot press.

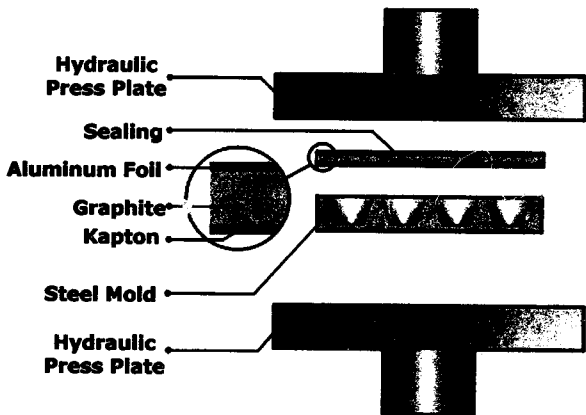


Figure 2-2: Schematic drawing of the setup for the steel mold and the gasket materials in the hot press (not to scale) [1].

To produce aerogels in the hot press, the following program was used:

Step	1	2	3	4	5	6
Temp (°F)	90	550	550	550	550	90
Pressure (psi)	550	550	550	150	150	150
Time (min)	2	240	30	30	30	240

Table 2-2: The parameters used for the closed-bottom mold in the hot press.

At the end of the program, the aerogels were removed from the mold and cut into smaller pieces using a razor blade. The original monoliths were roughly 25 mm in diameter and 15 mm thick. The smaller, monolithic pieces were then placed into 1.00-cm cuvettes for fluorescence measurements.

#### *Fabrication with Other Molds*

In order to optimize the fabrication process, several different molds and hot press programs were used to produce aerogels. One of the molds used was designed by Aaron Phillips and David Korin using SolidWorks computer software. This square, steel mold is pictured in Figure 2-3 below.

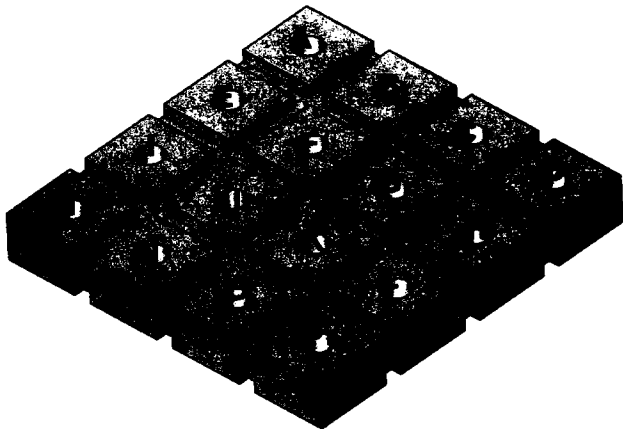


Figure 2-3: The square, steel mold used in the RSCE drying technique.

Unlike Bakrania's closed-bottom mold, the square mold has cavities that run completely through the mold. In addition, the square mold has smaller cavities, so the aerogel monoliths did not need to be broken in order to fit into cuvettes.

To produce aerogels in this mold, a similar procedure to the one described above was used. The only change was that the bottom of the mold had to be pre-sealed with the gasket materials before the precursor mixture was pipetted into the cavities. The mold was pre-sealed by placing a layer of aluminum foil on the bottom plate of the hot press. This was followed by a layer of graphite and then Kapton. The mold was then placed on top of the Kapton, followed by the three layers of gasket materials as depicted in Figure

2-2. Next, the steel mold was sealed at 700 psi for several minutes by closing the plates of the hot press. After the seal was allowed to form, the upper layer of gasket materials was removed, and the solution was transferred into the mold using a disposable glass pipet. The upper layer of gasket materials was replaced, and the hot press was programmed with the following set of parameters (Table 2-3).

Step	1	2	3	4
Temp (°C)	27	288	288	38
Pressure (psi)	720	720	150	150
Time (min)	2	210	30	180

Table 2-3: The parameters used in the hot press for the square mold.

The third mold used in this study was a round, steel mold. A diagram of this mold can be seen in Figure 2-4. Each hole in the round mold is at a geometrically equivalent position. Thus, ideally, the aerogels should be produced in equivalent environments.

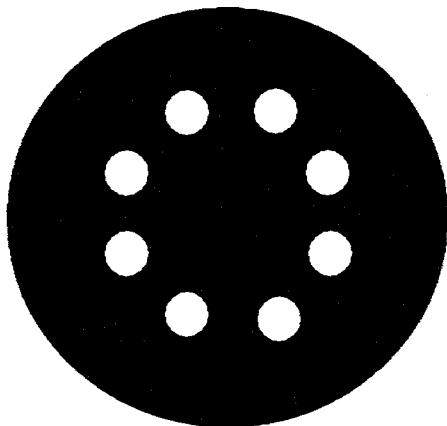


Figure 2-4: A top view of the round, steel mold used in the RSCE drying technique.

The procedure for this mold was the same as that for the square mold, except that a different set of hot press parameters was implemented (Table 2-4).

Step	1	2	3	4	5	6
Temp. (°C)	90	550	550	550	550	90
Pressure (psi)	1300	1300	1300	150	150	150
Time (min)	2	240	30	30	30	240

Table 2-4: The parameters used in the hot press for the round mold.

Lastly, the aerogels produced in the round mold had to be broken in order to fit into the 1.00-cm cuvettes. The original monoliths were approximately 15 mm in diameter and 20 mm thick.

### *Luminescence Measurements*

In order to measure the steady-state luminescence of the probe-doped aerogels, a Photon Technology International (PTI) fluorometer was used. This instrument included a model 814 Photomultiplier Detection System, and LPS-220B Lamp Power Supply, and an A-1010 Arc Lamp Housing. For most scans, 2-nm excitation and emission slits were all that was required to obtain an adequate signal. The excitation and emission wavelengths for PtTFPP were 387 nm and 650 nm. The excitation and emission wavelengths for PtOEP were 533 nm and 646 nm.

### *Time-based Luminescence Scans*

To analyze the responsiveness of the aerogels to changing oxygen concentrations, time-based luminescence scans were taken for each probe-doped gel. Using a gas proportioner, the amount of air and nitrogen gas flowing into the cuvette was varied over time. Table 2-5 shows the parameters for the time-based scans:

Time (min)	N <sub>2</sub> Reading	Air Reading	[O <sub>2</sub> ] (%)
0	0	100	21.5
5	20	80	17.2
10	40	60	12.9
15	60	40	8.6
20	80	20	4.3
25	100	0	0
30	80	20	4.3
35	60	40	8.6
40	40	60	12.9
45	20	80	17.2
50	0	100	21.5

**Table 2-5: The parameters used for varying the oxygen concentration during the time-based scans of each probe-doped aerogel. The readings correspond to the settings for the top ball on the gas proportioner.**

The computer program Kaleidagraph was then used to produce Stern-Volmer plots for these data. The data from the time-based scans was fit to the following equation:

$$y = I / [ (m_1 / (1 + m_2 * m_0)) + ((1 - m_1) / (1 + m_3 * m_0)) ] \quad [3]$$

where  $m_1 = f_1$  (fraction of the signal in one microenvironment),  $m_2 = K_{SV1}$ ,  $m_3 = K_{SV2}$  (Stern-Volmer quenching constants), and  $m_0 =$  percent oxygen. The starting conditions for the fit of this equation to the PtTFPP data were  $m_1 = 0.9$ ,  $m_2 = 1$ , and  $m_3 = 0.002$ . The starting conditions for the PtOEP fit were  $m_1 = 0.9$ ,  $m_2 = 60$ , and  $m_3 = 0.001$ .

#### *Luminescence Lifetime Scans*

The luminescence lifetimes of PtTFPP and PtOEP were compared by using the phosphorescence lifetime attachment of the spectrophotometer. The luminescence decay

curves for both probes were taken over a 700- $\mu$ s interval, and 10 scans were averaged. The estimated lifetimes for PtTFPP were 85  $\mu$ s and 20  $\mu$ s. The estimated lifetimes for PtOEP were 130  $\mu$ s and 100  $\mu$ s.

1. Gauthier, B. M.; Bakrania, S. D.; Anderson, A. M.; Carroll, M. K. *J. Non-Cryst. Solids*, 2004, 350, 238-43.
2. Lax, E. Spectroscopic investigation of the microenvironments experienced by rhodamine probes entrapped in silica aerogels and xerogels. Union College, June, 2005.
3. Demas, J. N.; DeGraff, B. A.; Coleman, P. B. *Anal. Chem.*, 1999, 71, 793A-800A.



## **Results and Discussion**

### ***Producing Uniform Samples***

From previous work by Aaron F. Phillips, I was aware that the square mold pictured in Figure 2-3, although an improvement on earlier designs, produced aerogels that lacked uniformity. In other words, the  $F_0/F$  ratios varied from sample to sample. This lack of uniformity is illustrated by the time-based scans and the  $F_0/F$  ratios of Phillips' 2-28-06 standard recipe PtOEP-doped aerogels (Figure 3-1 and Table 3-1). The letters C, H, I, J, and K in these figures correspond to unique cavities within the mold, as pictured in Figure 2-3.

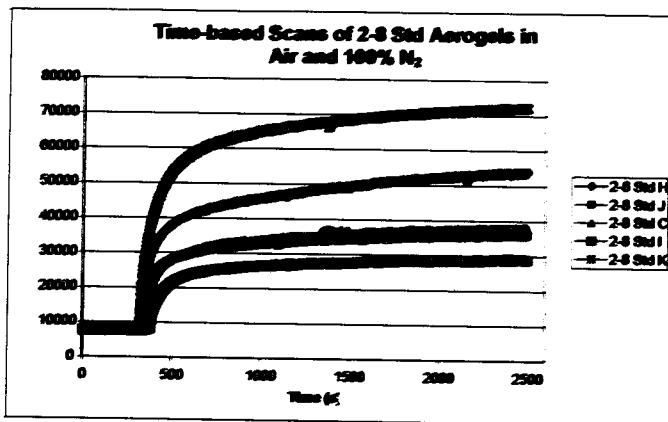


Figure 3-1: Time-based scan of Phillips' 2-28-06 standard recipe PtOEP-doped aerogels [1]. The data were collected using an excitation wavelength of 533 nm, an emission wavelength of 646 nm, and slit widths of 2 nm.

2-8 Sample	$\frac{F_{(100\% \text{ Nitrogen})}}{F_{(Air)}}$
C	5.0
H	6.5
I	3.6
J	4.5
K	8.8

Table 3-1:  $F_{\text{O}}/F$  ratios of Phillips' 2-28-06 standard recipe PtOEP-doped aerogels [1].

From Figure 3-1 and Table 3-1, one can see that the luminescence ratios are on the same order of magnitude. However, the highest value (8.8) differs from the lowest value (3.6) by approximately 60%. Hence, Phillips came to the conclusion that there was still room for improving the uniformity of the aerogels produced on the hot press.

When I first began producing gels, rather than continue with Phillips' mold, I decided to try producing aerogels in different molds. During one of the group meetings, it was suggested that the round mold (Figure 2-4) be used in place of the square mold. Unlike in the square mold, in the round mold the sol-gel samples are placed equal distances away from the center of the hot press, which the group believed represented environments that were more similar. Unfortunately, the round mold produced samples that were even less uniform than the samples shown in Figure 3-1. Figure 3-2 is a time-based scan of the 1-20-07 PtOEP-doped aerogels, and Table 3-2 is a summary of the  $F_0/F$  ratios of these samples.

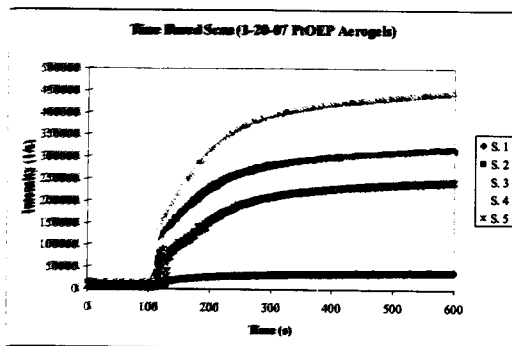


**Figure 3-2:** Time-based scans of the 1-20-07 PtOEP-doped aerogels produced in the round mold. The data was collected using an excitation wavelength of 533 nm, an emission wavelength of 646 nm, and slit widths of 2 nm. The samples were arbitrarily labeled S. 1 through S. 5 upon removal from the mold (see legend).

Sample	$F_0/F$
1	13.5
2	21.7
3	22.0
4	40.6
5	28.0

**Table 3-2:**  $F_0/F$  ratios of 1-20-07 PtOEP-doped aerogels produced in the round mold.

From Figure 3-2 and Table 3-1, it is evident that there is variation of the luminescence ratio between the samples. In addition, the highest value (40.6) differs from the lowest value (13.5) by 66.7%, which is larger than the difference between the high and low luminescence ratios of the samples produced in the square mold.

In addition, the 1-20-07 PtOEP-doped aerogels had many fissures, and could not be removed from the mold as monoliths. Overall, the samples from the round mold had more cracks and appeared to be less translucent than the gels prepared in the square mold. This could have been due to the higher restraining force required to seal the round mold. Later on, I learned that overfilling the cavities in the mold could also lead to fissures in the aerogels [2].

The next mold I decided to test was produced by Samirah Bakran in 2005 (Figure 2-1) [3]. This mold had a closed-bottom, and much larger cavities than Phillips' mold. Table 3-3 contains the  $F_0/F$  ratios obtained from a time-based scan of the 2-10-07 PtOEP-doped aerogels prepared in this mold.

Sample	$F_0/F$
1a	29.5
1b	24.2
2a	25.6
2b	27.3

Table 3-3:  $F_0/F$  ratios of 2-10-07 PtOEP-doped aerogels produced Bakran's mold. The data was collected using an excitation wavelength of 533 nm, an emission wavelength of 646 nm, and slit widths of 2 nm.

At first glance, these samples appeared to be much more uniform than the samples produced in the previous two molds. The visible qualities of these aerogels were also much better than previous samples. Aerogels produced in the closed-bottom mold had very few fissures, if any at all. They were also much more translucent than the round-mold and square-mold aerogels. When the highest luminescence ratio (29.5) is compared

to the lowest ratio (24.2), the difference is 18%. Since this mold appeared to produce the most uniform samples, I used it to prepare all of my subsequent batches of aerogels.

In addition, the closed-bottom mold offered a greater degree of control over the volume of precursor solution that was delivered to each cavity. In the previous two molds, leakage was a problem after the seal had been formed by the Kapton and graphite layers. As a result, it was virtually impossible to place equal volumes of solution into each of the cavities. This was not the case with Bakrania's mold. Initially, I did not pipette equal volumes into each space. Figure 3-3 is a time-based scan of the 2-3-07 PtTFPP-doped aerogels. When these aerogels were prepared, I filled the slots in the mold approximately two-thirds full. The  $F_0/F$  ratios for these samples are summarized in Table 3-4.

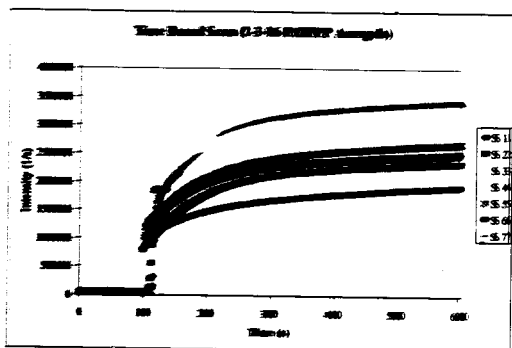


Figure 3-3: Time-based scans of the 2-3-07 PClFPP-doped acrygels. These gels were prepared in Bakracin's mold without volume control. The data was collected using an excitation wavelength of 367 nm, an emission wavelength of 650 nm, and slit widths of 2 mm.

Sample	$E_7/F$
1	64.2
2	82.6
3	109
4	78.6
5	75.4
6	87.6
7	85.6

Table 3-4: Luminescence ratios for the 2-3-06 PClFPP-doped acrygels.

Upon examining Figure 3-3 and Table 3-4, it appears that these samples show little improvement over the samples produced in the other molds. However, we observed that PClFPP-doped acrygels typically showed much greater  $E_7/F$  variation than the PClEP-

doped aerogels. This characteristic was perhaps inherent in the PtTFPP samples because their luminescence ratios were 3 to 5 times larger than the PtOEP samples, giving the PtTFPP samples a greater range over which to vary. When we compare the sample with the highest  $F_0/F$  ratio of the 2-3-07 PtTFPP-doped aerogels (109) to the sample with the lowest ratio (64.2), we see that these values differ by 41%. This is still a smaller percent difference than the other molds.

In order to test the effects of volume control, I prepared another batch of PtTFPP-doped aerogels in Bakrania's mold. Rather than estimate the volume of precursor solution I was entering into the mold's cavities, I pipetted exactly 4.50 mL of solution into each space (approximately two-thirds full). Table 3-5 contains the  $F_0/F$  ratios of the 2-10-07 PtTFPP-doped aerogels that were produced using volume control.

Sample	$F_0/F$
1a	51.0
1b	50.0
2a	74.6
2b	107

Table 3-5:  $F_0/F$  ratios of 2-10-07 PtTFPP-doped aerogels produced in Bakrania's mold using volume control.

From Table 3-5, the sample with the highest  $F_0/F$  ratio (107) differs from the sample with the lowest ratio (51) by 52%. Thus, there appears to be no significant improvement in sensor uniformity when volume control is used.



### *Time-Based Luminescence Scans of Aerogels Produced Via the RSCE Method*

One desirable characteristic of a probe-doped gas sensor is sensitivity towards the analyte molecule. In this case, the greater response to changing oxygen concentrations, the more sensitive a probe is to oxygen. In addition, the more sensitive a probe is to oxygen, the more suitable the probe is for sensing oxygen. In order to compare the sensitivities of PtOEP and PtTFPP, time-based scans of these aerogels were taken in varying concentrations of oxygen. The data from these time based scans were then used to generate Stern-Volmer (S-V) plots, which allowed me to quantitatively compare the sensitivities of each probe-doped aerogel.

Since the aerogels produced in Bakrania's mold were generally the most uniform, I decided to use these samples as a basis for comparing PtOEP and PtTFPP. First, time-based scans were taken for samples of each probe-doped aerogel. Figures 3-4 and 3-5 are time-based scans of the 2-10-07 PtOEP- and PtTFPP-doped aerogels respectively. The air and nitrogen proportion flowing into the cuvette during the scan was changed every 200 s.

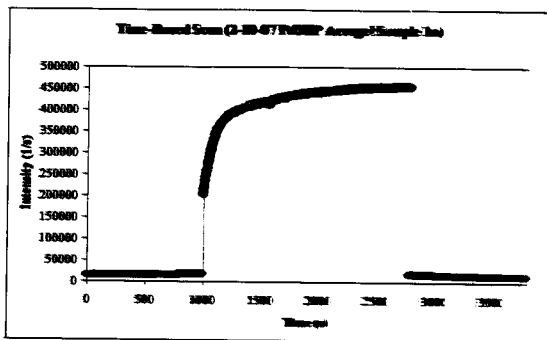


Figure 3-4: Time-based scan of 2-10-07 P(PEP)-doped sample 1a. The data was collected using an excitation wavelength of 533 nm, an emission wavelength of 636 nm, and slit widths of 2 nm.

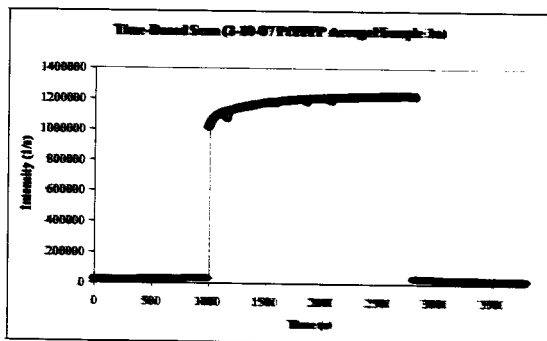
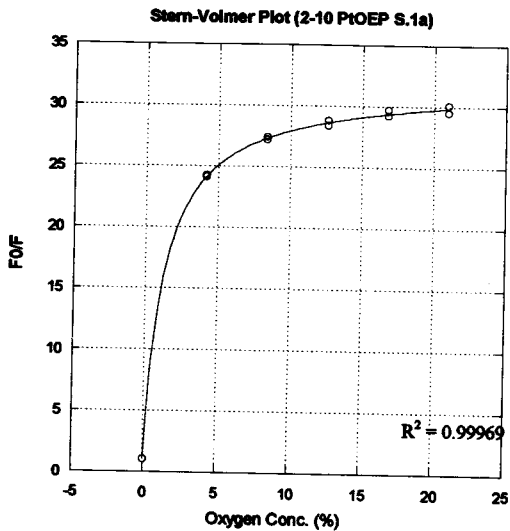


Figure 3-5: Time-based scan of 2-10-07 P(HTP)-doped sample 1a. The data was collected using an excitation wavelength of 367 nm, an emission wavelength of 630 nm, and slit widths of 2 nm.

Once the aerogels were in 100% nitrogen, they began to approach their maximum luminescence intensity. However, once a certain level of intensity was reached, the signal approached its maximum very slowly. As a result, the samples were allowed 1800 s to achieve their highest level of luminescence intensity. Figures 3-6 and 3-7 are S-V plots of the 2-10-07 PtOEP- and PtTFPP-doped aerogels respectively. Both the PtOEP- and PtTFPP-doped gels were fit with a two-site S-V equation, because previous research had shown that the probes existed in more than one microenvironment within the aerogel matrix [4].



**Figure 3-6:** S-V plot for 2-10-07 PtOEP-doped aerogel sample 1a. The equation to the line is  $y = 1/[(f/(1+K_{SV1}*[O_2])) + ((1-f)/(1+K_{SV2}*[O_2]))]$ . For this sample,  $f = 0.968$ ,  $K_{SV1} = 23.9$ , and  $K_{SV2} = 5.56 \times 10^{-4}$ .

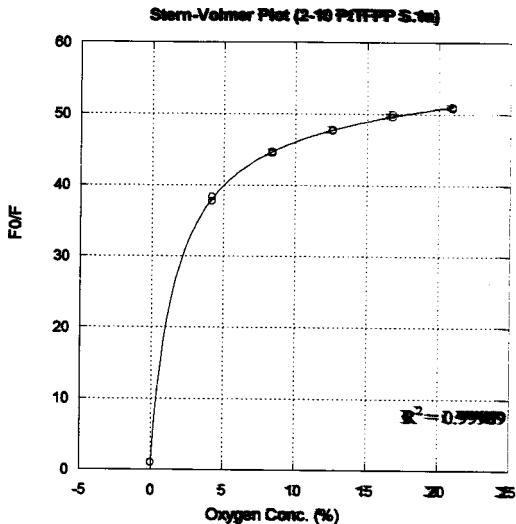


Figure 3-7: S-V plot for 2-10-07 PtTFPP-doped aerogel sample 1a (the vertical line is an artifact). The equation to the line is  $y = 1 / [ (f(1 + K_{SV1} * [O_2])) + ((1-f)(1 + K_{SV2} * [O_2])) ]$ . For this sample,  $f = 0.981$ ,  $K_{SV1} = 30.7$ , and  $K_{SV2} = 2.19 \times 10^3$ .

From the S-V plots, I obtained the fraction of the probe in one of the microenvironments ( $f$ ), the R-squared value of the fit, and the S-V quenching constants for the probe in each microenvironment ( $K_{SV1}$  and  $K_{SV2}$ ). These data are summarized in Table 3-6 for the PtOEP-doped aerogels, and in Table 3-7 for the PtTFPP-doped aerogels.

Sample	f	$K_{SV1}$	$K_{SV2}$	$R^2$
1a	0.968	23.9	$5.56 \times 10^{-4}$	0.99969
1b	0.958	29.9	$2.48 \times 10^{-3}$	0.99981
2a	0.962	27.4	$2.74 \times 10^{-3}$	0.99842
2b	0.963	28.8	$2.68 \times 10^{-3}$	0.99981
Average	0.963	27.5	$2.11 \times 10^{-3}$	0.99943

Table 3-6: Summary of the S-V data for the 2-10-07 PtOEP-doped aerogels.

Sample	f	$K_{SV1}$	$K_{SV2}$	$R^2$
1a	0.981	30.7	$2.19 \times 10^{-3}$	0.99989
1b	0.980	36.4	$2.46 \times 10^{-3}$	0.99996
2a	0.988	54.7	0*	0.99958
2b	0.991	47.6	$9.82 \times 10^{-4}$	0.99970
Average	0.985	42.4	$1.41 \times 10^{-3}$	0.99978

Table 3-7: Summary of the S-V data for the 2-10-07 PtTFPP-doped aerogels. \*The  $K_{SV2}$  for sample 2a is listed as 0 because the actual value obtained from the plot was  $-5.10 \times 10^{-4}$ , a nonsensical result. Thus, it was assumed that the actual value for this constant was zero.

From the average values of  $K_{SV1}$ , one can see that the PtTFPP-doped aerogels had overall higher quenching constants in microenvironment 1 (where the majority of the probe was located). According to the average  $K_{SV1}$  values, the PtTFPP-doped aerogels were more sensitive to changing oxygen concentrations. With respect to sensitivity, PtTFPP appears to be a better oxygen sensor than PtOEP. For both probes, the  $K_{SV2}$  values were very close to zero, which indicates either that the probe is inaccessible to

oxygen or that it is bound to the aerogel matrix in such a way that it no longer interacts with oxygen.

*Time-Based Luminescence Scans of Aerogels Produced Via the Conventional (Autoclave)*

*Method*

To compare the probe-doped aerogels made via RSCE to the probe-doped aerogels made in the autoclave, time-based scans were taken for PtOEP- and PtTFPP-doped autoclave aerogels prepared by Amanda Barrow. One marked difference between the autoclave and the RSCE aerogels was the  $F_0/F$  ratio. For both probes, the autoclave produced aerogels with much lower  $F_0/F$  ratios. The  $F_0/F$  ratios for the PtOEP- and PtTFPP-doped autoclave aerogels can be viewed in Tables 3-8 and 3-9, respectively.

Sample	$F_0/F$
1	10.8
2	11.9
3	13.2
4	8.00
5	12.8
6	10.4

Table 3-8:  $F_0/F$  ratios of the 2-4-07 PtOEP-doped aerogels produced in the autoclave. These aerogels were prepared using solvent rinses containing PtOEP, so less leaching of the probe was observed than for other batches.

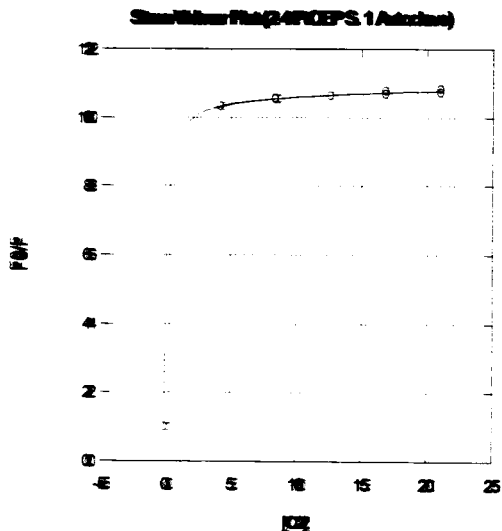
Sample	F <sub>0</sub> /F
1	1.76
2	1.65
3	1.78
4	1.68
5	1.77
6	1.59

Table 3-9: F<sub>0</sub>/F ratios of the 2-1-07 PtTFPP-doped aerogels produced in the autoclave.

Solvent rinses used in preparing this sample did not include the probe. Significant leaching of probe from the wet gel occurred.

From the time-based scans of each probe-doped aerogel, S-V plots were produced. An example of one of these S-V plots is shown in Figure 3-8. From these plots, we were able to obtain the K<sub>SV</sub> values for each aerogel. Tables 3-10 and 3-11 contain the S-V data for the PtOEP- and PtTFPP-doped autoclave aerogels, respectively.





**Figure 3-8** S-N plot for 2.407 PDEP-doped aerogel sample 1, which was produced in the annealer. The equation to the line is  $y = 1 / [((1 + K_{sv1} * [O_2]) + ((1 - f) * (1 - K_{sv2} * [O_2])))]$ . For this sample,  $f = 0.968$ ,  $K_{sv1} = 23.9$ , and  $K_{sv2} = 5.56 \times 10^{-4}$ .

Sample	f	$K_{SV1}$	$K_{SV2}$	$R^2$
1	0.906	65.0	$9.35 \times 10^{-4}$	0.99993
2	0.916	40.6	$4.40 \times 10^{-4}$	0.99991
3	0.924	81.1	$1.03 \times 10^{-3}$	0.99977
4	0.875	32.3	$6.11 \times 10^{-4}$	0.99998
5	0.922	61.0	$9.85 \times 10^{-4}$	0.99944
6	0.906	50.7	$4.59 \times 10^{-4}$	0.99911
Average	0.908	55.1	$7.43 \times 10^{-4}$	0.99969

Table 3-10: Summary of the S-V data for the 2-4-07 PtOEP-doped aerogels produced in the autoclave.

Sample	f	$K_{SV1}$	$K_{SV2}$	$R^2$
1	0.404	2.50	$2.44 \times 10^{-3}$	0.99673
2	0.361	3.80	$2.51 \times 10^{-3}$	0.99914
3	0.374	10.6	$4.35 \times 10^{-3}$	0.99282
4	0.352	5.08	$3.95 \times 10^{-3}$	0.99818
5	0.387	4.91	$3.38 \times 10^{-3}$	0.99519
6	0.33	3.52	$3.74 \times 10^{-3}$	0.9982
Average	0.368	5.07	$3.39 \times 10^{-3}$	0.99671

Table 3-11: Summary of the S-V data for the 2-1-07 PtTFPP-doped aerogels produced in the autoclave.

When comparing the S-V data of the autoclave aerogels to the S-V data of the RSCE aerogels (Tables 3-6 and 3-7), there appear to be a few inconsistencies. For instance, the  $K_{SV1}$  values of the PtOEP-doped RSCE aerogels are roughly half the  $K_{SV1}$  values for the PtOEP-doped autoclave aerogels. In contrast, the PtTFPP-doped RSCE aerogels have  $K_{SV1}$  values that are approximately six times larger than the  $K_{SV1}$  values for the PtTFPP-doped autoclave aerogels. Thus, there appears to be no relationship between the processing

method and the  $K_{SV1}$  values for each probe-doped aerogel. However, it can be noted that for both probes, the fraction in the microenvironment more responsive to oxygen ( $f$ ) was higher for the RSCE aerogels. Hence, it appears that the RSCE method produces aerogels with a more uniform microenvironment. Lastly, by examining Tables 3-8 and 3-9, and comparing them to the  $F_0/F$  ratios of aerogels produced via RSCE, it becomes evident that the RSCE method produces aerogels with a larger  $F_0/F$ . Even when the autoclave aerogels were prepared using solvent rinses that contained the probe, the  $F_0/F$  ratios were still smaller than the  $F_0/F$  ratios of the RSCE aerogels. Essentially, the data above suggests that the RSCE method produces comparable, if not better quality aerogels, than the conventional method if we define quality aerogels as having high  $F_0/F$  ratios, high  $K_{SV1}$  values, and uniform microenvironments.

#### *Luminescence Lifetime Studies*

In order for a probe to be an effective gas sensor, it must have a long luminescence lifetime ( $>10$  ns) [5]. Probes with shorter lifetimes lose their energy before the quenching species (oxygen) has time to interact with the excited state luminophore. In contrast, probes with longer lifetimes give the quenching species more time to interact with the excited state luminophore, giving the luminophore a greater ability to report on quencher concentration. In this section of my study, I compared the lifetimes ( $\tau_0$ ) of the PtOEP- and PtTFPP-doped aerogels prepared on 2-10-07. Figures 3-9 and 3-10 are the luminescence decay scans for a PtOEP- and PtTFPP-doped aerogel respectively.

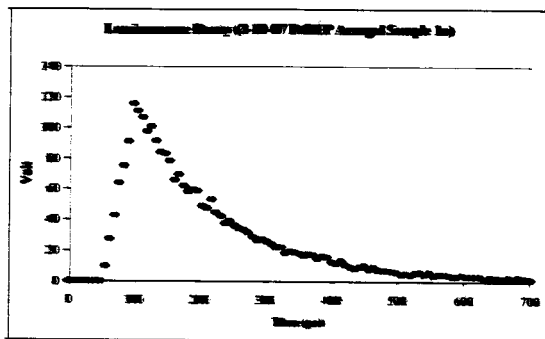


**Figure 3-9: Luminescence decay scan for 2-10-07 P(O)EP sample 1a. The data was collected using an excitation wavelength of 533 nm, an emission wavelength of 646 nm, and slit widths of 2 nm. In addition, the data was taken over a 700-ps interval, and was averaged over 10 scans.**

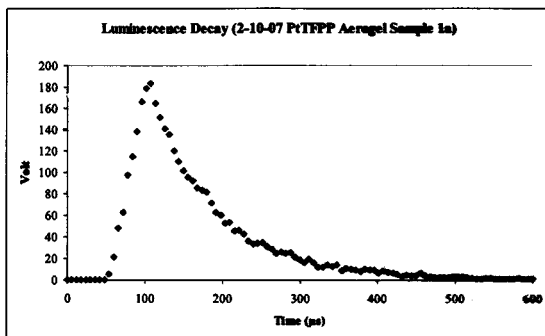


Figure 3-10: Luminescence decay scan for 2-10-07 PtTFPP aerogel sample 1a. The data was collected using an excitation wavelength of 387 nm, an emission wavelength of 650 nm, and slit widths of 3 nm. In addition, the data was taken over a 700- $\mu$ s interval, and was averaged over 10 scans.

By scanning the luminescence decay for all of the PtOEP and PtTFPP aerogels, I was able to determine the lifetimes of each probe. The lifetime data and the chi-squared values for the PtOEP- and PtTFPP-doped aerogels can be found in Tables 3-12 and 3-13 respectively.

Sample	$\tau_1$ ( $\mu\text{s}$ )	$\tau_2$ ( $\mu\text{s}$ )	$\chi^2$
1a	140.1	18.12	1.001
1b	138.2	7.937	0.8502
1c	132.1	28.13	0.8805
1d	127.2	125.7	0.7636
2a	115	111.3	0.8801
2b	421.3	71.38	1.127
2c	160.2	18.73	1.362
2d	254.7	61.97	0.7925
Average	200	60	
Std. Dev.	100	50	

Table 3-12: Luminescence lifetime data for the 2-10-07 PtOEP-doped aerogels.

Sample	$\tau_1$ ( $\mu\text{s}$ )	$\tau_2$ ( $\mu\text{s}$ )	$\chi^2$
1a	83.15	7.892	1.011
1b	85.67	4.398	1.089
1c	85.09	1.939	1.05
1d	86.17	1.74	0.7381
2a	79.15	8.126	0.7959
2b	78.83	6.972	0.8523
2c	85	6.743	1.467
2d	84.83	2.963	0.7621
Average	84	5	
Std. Dev.	3	3	

Table 3-13: Luminescence lifetime data for the 2-10-07 PtTFPP-doped aerogels.

When comparing the average lifetime values for each probe-doped aerogel, one can see that the PtOEP samples have much longer luminescence lifetimes. However, the chi-squared values for most of the fits to the decay curves are poor. Even though they can

still provide us with a qualitative basis for comparison, it is difficult to determine the true lifetimes of the probes from this data alone.

1. Phillips, A. F. "Fabrication and Characterization of PtOEP-doped Silica Aerogels with Varied Amounts of Water for Use as Oxygen Sensors." Union College, June, 2006.
2. Anderson, A. M. Personal communication. Union College, February, 2007.
3. Smiteah, B. "Characterization of Silica-Aerogels Fabricated using a Novel Processing Technique." Union College, March, 2003.
4. Plata, D. L.; Briones, Y. J.; Wolfe, R. L.; Carroll, M. K.; Bakravin, S. D.; Mandel, S. G.; Anderson, A. M. *J. Non-Cryst. Solids*. 2004, 350, 326-35.
5. Demas, J. N.; DeGraff, B. A.; Coleman, P. B. *Anal. Chem.* 1999, 793A-800A.

## Conclusions

By changing the mold that was originally used by Phillips to produce aerogels, it appears that we have found a way to produce aerogels that are more uniform in their luminescence signal. Phillips' square mold yielded aerogels with  $F_0/F$  ratios that showed a 60% difference between the sample with the highest ratio and the sample with the lowest ratio. For aerogels produced in the round mold, this difference was 67%. However, for aerogels produced in the closed-bottom mold, this difference was only 18%. By creating aerogels with more uniform  $F_0/F$  ratios, stronger conclusions can be made about the effectiveness of a processing method and the characteristics of different probes. Thus, if signal uniformity is the goal, the closed-bottom mold appears to be the best mold for producing aerogels.

When comparing the PtOEP- and PtTFPP-doped RSCE aerogels, we determined that PtTFPP had a higher  $K_{SV1}$  value (42.4) than PtOEP (27.5). From this data we concluded that PtTFPP was the more sensitive probe. In industry, probes with greater sensitivities are more desirable, as they can detect finer changes in their environment. Therefore, with respect to this criterion, it appeared that PtTFPP was a better oxygen sensor than PtOEP. However, when luminescence lifetimes were taken for each probe-doped aerogel, we found that PtOEP had an average  $\tau_1$  of 186  $\mu\text{s}$ , whereas PtTFPP had an average  $\tau_1$  of 83.5  $\mu\text{s}$ . Typically, probes with longer lifetimes are more desirable because they remain in the excited state longer, allowing them more time to interact with the analyte molecule (the quencher). Hence, with respect to luminescence lifetimes, PtOEP appeared to be the better probe. Yet, from past studies in our group, we had learned that PtOEP was subject to photodecomposition, meaning that it would lose its ability to



respond to oxygen after long term exposure to light [1]. PtTFPP, on the other hand, did not exhibit this behavior. Thus, we concluded that PtTFPP was overall a more reliable oxygen sensor than PtOEP.

Lastly, we were able to make some preliminary comparisons between the RSCE method and the conventional method through the use of SV analysis. In general, aerogels produced via RSCE had  $F_0/F$  ratios that were much higher than aerogels produced in the methanol. The SV data showed that the RSCE method and the conventional method produced aerogels with comparable  $K_{SV}$  values as well. Furthermore, in regards to the conventional method, the effect of solvent rinses containing the probe appeared to be significant. When the solvent rinses contained the probe,  $F_0/F$  ratios and  $K_{SV}$  values seemed to be larger. Still, even when solvent rinses contained the probe, the conventional method produced  $K_{SV}$  values that were not significantly larger than the  $K_{SV}$  values for the RSCE aerogels. Finally, when we consider the fact that the conventional method can typically take days to make aerogels, and the RSCE method only takes hours, it appears that RSCE method is more efficient since it can produce aerogels of comparable quality in a fraction of the time. However, future studies in this area must be done until we can conclusively comment on the efficiency and effectiveness of the RSCE method over the conventional method.

1. Phillips, A. F. "Fabrication and Characterization of PtOEP-doped Silica Aerogels with Varied Amounts of Water for Use as Oxygen Sensors." Union College, June, 2006.

## Acknowledgments

I would first like to thank Professor Mary Carroll for her support and guidance. Without her wisdom and resources, much of this research would not have been possible. I would also like to acknowledge Professor Ann Anderson for the insight she provided into operating and optimizing the hot press.

I am indebted to the entire Union College acrogel team of students, past and present. I thank Aaron Phillips ('06) and Smitesh Bakrania ('08) for their past efforts, which became the groundwork for my research. I must also thank Jessica Beardsland ('07) and Amanda Barrow ('08) for their help in the lab.

For funding, I thank the NSF MRI grant for lab instrumentation, the NSF EEC grant, and the Union College Internal Education Fund for travel support to the NCLER meeting in California.

Lastly, I would like to thank my family for supporting my endeavors as an undergraduate, and for giving me the opportunity to attend Union.